Morphology-Controllable Synthesis of Pyrene Nanostructures and Its Morphology Dependence of Optical Properties

Xiujuan Zhang,[†,§] Xiaohong Zhang,[*,†] Wensheng Shi,[†] Xiangmin Meng,[†] Chunsing Lee,[‡] and Shuittong Lee[*,†,‡]

Nano-Organic Photoelectronic Laboratory, Technical Institute of Physics and Chemistry, Chinese Academy of Sciences, Beijing 100101, China and Center of Super-Diamond and Advanced Films (COSDAF), City University of Hong Kong, Hong Kong SAR, China

Received: May 8, 2005; In Final Form: July 27, 2005

Morphology-controllable synthesis of various pyrene nanostructures from nanoparticles to short nanorods and nanowires (long nanorods) was achieved by a simple self-assembly method. In this approach, aqueous sodium dodecyl sulfate (SDS) micelles were used as templates to direct the self-assembly of the pyrene molecules into nanorods. It was found that changing the concentration ratio of the pyrene to SDS molecules could be employed to control the aspect ratio (length to diameter) of the pyrene nanostructures from 1 to 50 or higher. Moreover, the dimensional variation was accompanied by changes of their optical properties. With the increase of the aspect ratio, the characteristic fluorescence of the isolated pyrene molecules was suppressed and concurrently replaced by the excimer emission of the pyrene nanostructures. A blue-shift was observed in the excimer emission peaks as the length of the nanorods increased. The growth mechanism and the change in optical properties of these pyrene nanostructures were discussed in detail.

Introduction

In recent years, nanostructures of small-molecule organic materials have attracted a great deal of excitement in the development of novel optoelectronic devices due to their low production cost and tunable electronic and optical properties.[1−4] Properties of organic nanostructures are expected to be sensitively dependent on both shapes and sizes. The size dependence of the optical properties has been widely studied in organic nanostructures, such as nanoparticles, nanowires, and nanotubes, and the results showed an exciting potential of property tunability.[5−8] However, there are relatively little reports on the synthesis of organic nanostructures with custom controlled morphologies and the dependence of their corresponding properties on unique morphologies. In this work, a self-assembly method was introduced to readily produce pyrene nanorods with select aspect ratios (nanoparticles, short nanorods, and nanowires) via controlling the variation of the concentrations of the source materials. It was observed that the pyrene nanostructures with different aspect ratios performed distinct optical properties. This approach provided a simple and rational way to custom tune the optical properties of organic nanostructures through modifying morphology. To the best of our knowledge, it is the first report about the morphology-controllable synthesis of organic nanostructures based on small molecular materials and its corresponding morphology dependence of optical properties. Moreover, in our recent work, it has been proved that the self-assembly method is applicable to other aromatic π-conjugated organic molecular systems with relatively planar structures, such as some highly important organic optoelectronic materials: perylene, pentacene, etc.[9]

Experimental Section

Materials. Pyrene and sodium dodecyl sulfate (SDS) were purchased from ACROS and used without further treatment. Ethanol was obtained from Beijing Chemical Agents. Ultrapure water with a resistivity of 18.2 MΩ cm was produced using a Milli-Q apparatus (Millipore) and was filtered using an inorganic membrane with a pore size of 0.02 μm (Whatman International, Ltd.) just before use.

Preparation. Pyrene nanostructures were prepared by a self-assembly method using SDS micelles as templates. A pyrene/ethanol solution (1.8×10^{-3} mol L^{-1}) in 50, 100, and 200 μL samples, labeled as A, B, and C, respectively, was individually injected drop-by-drop into 5 mL of SDS micelle aqueous solution (3.6×10^{-3} mol L^{-1}) and stirred for 5 min. The samples were then left standing for 10−30 min for stabilization. Afterward, sample A showed no observable changes, whereas samples B and C showed a white and cloudy feature, and the extent of cloudiness further increased in sample C. If 100 μL of pyrene/ethanol solution (1.8×10^{-3} mol L^{-1}) was injected into 5 mL of SDS micelle aqueous solutions with a concentration of 7.2×10^{-3} mol L^{-1}, 3.6×10^{-3} mol L^{-1}, and 1.8×10^{-3} mol L^{-1}, samples D, E, and F were obtained, which respectively showed similar properties to samples A, B, and C, having correspondingly the same final concentrations.

Characterization. The morphologies of the nanostructures were observed with a field-emission scanning electron microscope (FESEM, Hitachi S-4300), operated at an accelerating voltage of 5 kV. A few drops of each sample were placed onto silicon substrates for SEM examination. To eliminate the influence of the SDS on above characterization, the specimens

* Corresponding authors. E-mail: apannale@cityu.edu.hk (S.T.L.); xhzhang@mail.ipc.ac.cn (X.H.Z). Fax: +852-27844696 (S.T.L.). Telephone: +86-10-64888169 (X.H.Z.).

† Nano-Organic Photoelectronic Laboratory, Technical Institute of Physics and Chemistry.

‡ Center of Super-Diamond and Advanced Films (COSDAF), City University of Hong Kong.

§ Dr. Xiujuan Zhang is also in the Graduate School of the Chinese Academy of Sciences, Beijing 100039, People's Republic of China.

10.1021/jp052385j CCC: $30.25
Published on Web 09/16/2005

were mildly rinsed with ultrapure water and air-dried. To minimize sample charging, a thin layer of Au was deposited onto the samples for SEM examination. The samples without Au coating were characterized with fluorescence microscopy (OLYMPUS -1×17). UV−vis absorption spectra of the pyrene nanostructures dispersed in an aqueous surfactant system and pyrene/alcohol solution (1×10^{-5} mol L^{-1}) were measured using a Hitachi U-3010 spectrophotometer. Photoluminescence (PL) spectra were recorded with a Hitachi F-4500 spectrometer at an excitation wavelength of 340 nm. Fluorescence anisotropy of the samples was measured with a Hitachi MPF-4 spectrometer. Time-resolved fluorescence measurements were carried out under ambient conditions using a time-correlated single-photon counting (TCSPC) spectrometer (Edinburgh Instrument F 900) with the detection wavelength at 465, 471, and 476 nm respectively for samples A, B, and C and the excitation wavelength at 340 nm for all.

Results and Discussion

SEM micrographs of the nanostructures are shown in Figure 1. In the SEM micrograph (Figure 1a) of sample A, only nanoparticles with sizes of about 150 nm were observed. As the concentration of pyrene increases from sample A to C, the nanoparticles elongate to become nanorods of about 3−5 μm in length and 150 nm in diameter (Figure 1c), and the corresponding aspect ratio changed from 1 to 50 or higher. It is significant to note that the increase of the pyrene concentration leads to size increase mainly in one dimension, with little change in the diameter of the rod. To confirm that the nanostructures are composed of the pyrene instead of SDS molecules, the corresponding fluorescence microscopic studies were carried out. The fluorescence micrographs show similar microstructures to that observed in the SEM (see Supporting Information). As the surfactant molecules exhibit hardly any fluorescence, it was reasonably deduced that the nanostructures observed in SEM were composed mainly of the pyrene molecules. In addition, after redissolution of the filtered nanorods by solvent, the corresponding nuclear magnetic resonance (NMR) and mass spectroscopy (MS) results additionally confirmed that the composition of the nanorods was pyrene molecules.

To further understand the role of surfactant in the formation of nanostructures, experiments were repeated by injecting the pyrene/ethanol solution into water instead of the SDS surfactant. In this case, only nanoparticles were observed, irrespective of the amount of pyrene/ethanol injected into water. This result verifies the critical role of the SDS micelles on the aggregation of the pyrene molecules. It also provides a basis to understand the formation mechanism of pyrene nanostructures with different morphologies under different conditions, which is illustrated in Scheme 1. First, in the initial stage, the hydrophobicity of the pyrene molecule would facilitate its entrance into the hydrophobic core sphere of the SDS micelles. When only a few pyrene molecules are present in the system, all of them could disperse into the core of the micelles where the alkyl chains of SDS would separate the pyrene molecules from each other and prevent them from aggregating. Thus, a thermodynamically stable system is formed under a low pyrene concentration. As the pyrene concentration increases in the surfactant aqueous solution, more and more pyrene molecules have to squeeze into one micelle. The over-accommodated micelle would eventually become energetically unfavorable, and the SDS molecules in the micelle would not be sufficient to completely enclose the pyrene molecules. Instead, the micelle would only partially protect the already-formed microcrystals of the preexisted pyrene molecules. The strong $\pi-\pi$ stacking interactions between adjacent pyrene molecules would facilitate the molecules stacking onto one another. Therefore, the $\pi-\pi$ interactions

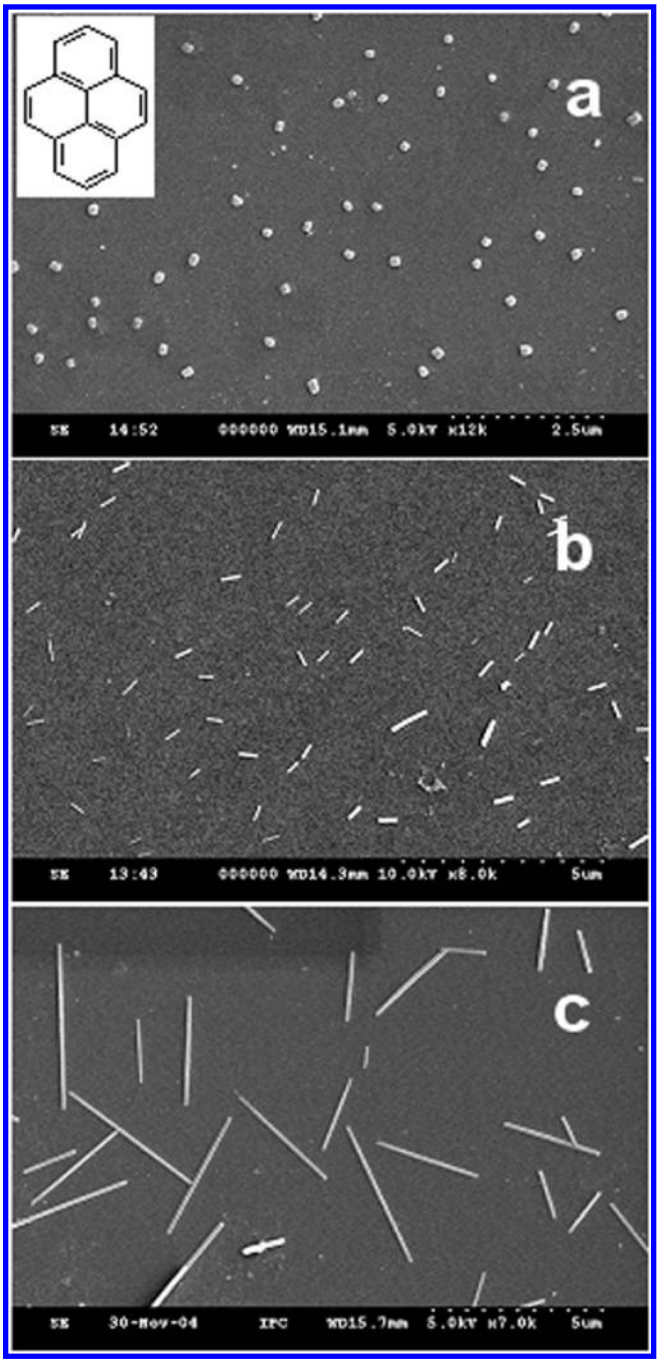

Figure 1. FESEM images of pyrene nanostructures of different morphologies (a) nanoparticles labeled as sample A, (b) short nanorods labeled as sample B, (c) nanowires (long nanorods) labeled as sample C. Inset in (a) shows the molecular structure of pyrene.

SCHEME 1: Possible Formation Processes of Organic Nanostructures of Different Morphologies

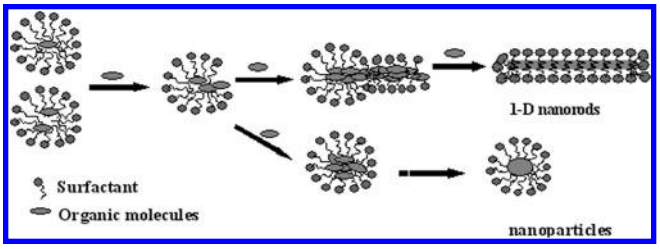

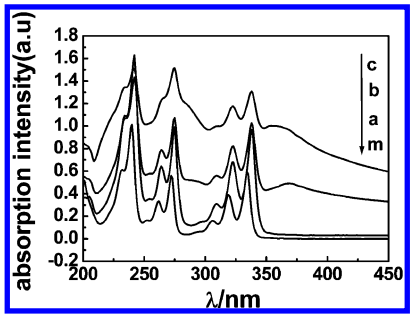

Figure 2. UV−visible absorption spectra of pyrene nanostructures (lines a−c for samples A−C, respectively) and the pyrene/ethanol dilute solution (1.0×10^{-5} mol L^{-1}) (line m).

would provide the dominant stacking direction, while the surfactant would give the vital protection. As a result, the pyrene aggregates would be confined to grow mainly along the normal direction of the molecular plane. According to this growth model, the aspect ratio of the nanostructures would be directly controlled by the concentration ratio of the pyrene to SDS molecules. This deduction is indeed confirmed by our observation that pyrene nanorods with different aspect ratios can be reproducibly obtained by changing the SDS concentration while keeping the pyrene/ethanol concentration constant.

Figure 2 shows UV−vis absorption spectra of the as-prepared pyrene nanostructures (curves a−c) and the pyrene/ethanol dilute solution (curve m). The absorption peaks of the pyrene nanostructures are red-shifted and broadened compared with those of the diluted solution. Furthermore, a new band of the nanostructures centered at 360 nm emerges, which is not observed in the dilute solution. It suggests that this new band originates from the aggregated pyrene molecules.[10−11] This band becomes increasingly prominent as the nanoparticles grow (curve a) into nanorods (curve b), and eventually into nanowires (long nanorods) (curve c). In addition, the trailing edge of the spectra at longer wavelengths becomes more pronounced for the nanorods than for the nanoparticles due to the Mie scattering effect.[12]

Figure 3a shows the fluorescence excitation spectra of the pyrene nanostructures (lines a−c). From the spectra, we can also see the gradual emergence of a new band at the longer wavelength similar to the observation in the absorption spectra (Figure 2). Figure 3 b shows the emission spectra of the pyrene nanostructures (curves a−c) and the diluted (1.0×10^{-5}mol L^{-1}) pyrene/ethanol solution. The diluted solution exhibits the characteristic pyrene monomer emission, showing a few peaks and the fine structures in the range of 370−410 nm. For comparison, we also examined the emission from the concentrated solution and the bulk solid (emission spectra are shown in Supporting Information). In the concentrated pyrene/ethanol solution (1.8×10^{-3} mol L^{-1}), besides the emission of the monomer, the excimer emission emerges near 470 nm, although with relative weak intensity. The bulk pyrene solid only shows strong broad excimer emission from 420 to 500 nm. However, as illustrated in Figure 3b, the emission spectra of the pyrene nanostructure suspensions exhibit two distinct regions originating respectively from the monomer (370−410 nm) and excimer (420−500 nm) emission. The monomer emission is strongly quenched by the excimer emission at the nanostructures. As the nanorods grow in length, the excimer emission shows a blue-shift from 476 nm (curve a) to 471 nm (curve b), and then to 465 nm (curve c). The blue-shift may be attributed to the difference in aggregation modes of pyrene molecules in different nanostructures. This is similar to that identified in naphthalene aggregates, in which two naphthalene molecules stacking on

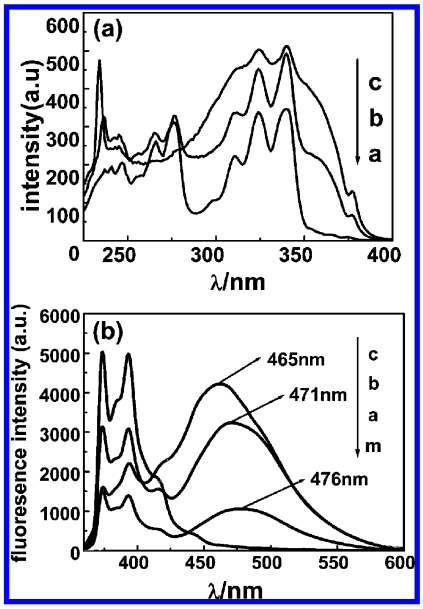

Figure 3. (a) Fluorescence excitation spectra of pyrene nanostructures. Lines a−c are for samples A−C, respectively ($\lambda_{em} = 470$ nm). (b) Emission spectra for different samples. Lines a, b, and c are for samples A, B, and C, respectively, and m for the dilute pyrene/ethanol solution (1.0×10^{-5} mol L^{-1}) ($\lambda_{ex} = 340$ nm).

TABLE 1: Key Physical Data of These Three Samples

sample	r[a]	τ (ns)[b]	I_{m3}/I_{m1}[c]	I_e/I_{m1}[d]
A	0.014	50.6	0.72	0.69
B	0.022	43.1	0.76	1.04
C	0.034	40.2	0.99	2.58

[a] Fluorescence anisotropy (r). [b] Fluorescence lifetime (τ). [c] The ratio of I_{m3}/I_{m1}. [d] The ratio of I_e/I_{m1}.

each other in different fashions would lead to the shift of the emission peak.[13]

It is worthwhile to note that, when larger volumes of pyrene/ethanol solution are used than that in sample C to get larger or longer nanowires, the corresponding emission no longer exhibits an obvious blue-shift compared with that of sample C. It can be considered that the spectroscopic property would not be influenced any more after having the proper arrangement of molecular aggregations. Furthermore, the emission peak width also gradually decreases with increasing aspect ratio of the nanorods, which suggests that molecular arrangement in the nanorods becomes more regular.[14−16] The fluorescence polarization of the samples further elucidates this presumption. The pyrene/ethanol solution has zero fluorescence anisotropy due to the random tropism of the molecules, whereas the samples A, B, and C show fluorescence anisotropy (r), which increase as the nanorods grow longer. The results are listed in Table 1. This again confirms that the packing constraint and orientation of the molecules becomes more prominent, with nanoparticles gradually growing into one-dimensional nanowires. Fluorescence lifetimes (τ) of the pyrene nanorod suspensions with different aspect ratios were measured with an excitation of 340 nm at ambient conditions (Table 1). The fluorescence lifetime of pyrene in ethanol solution is 18.5 ns, whereas that of the pyrene nanorod suspensions decreases from 50.6 to 40.2 ns, i.e., the fluorescence decay process is accelerated as the aspect ratio increases. The longer lifetimes of pyrene nanorods compared with that of pyrene in ethanol solution are easily understood in that the formation of nanorods restricts the rotation and vibration of molecules and thus increases the emission lifetime.[8]

It has been reported that the intensity ratio of the third (384 nm) to the first (373 nm) emission peaks (I_{m3}/I_{m1}) of the pyrene solution increases as the environmental polarity decreases.[17−18] As expected, this ratio would similarly increase as the nanorods grow (Table 1). The intensity ratio of the excimer-to-monomer emission (I_e/I_{m1}) also increases as the rods grow. These also indicate that the packing constraint increases from samples A to C as more molecules segregate in the formation of nanocrystals.

Conclusion

In summary, pyrene nanorods with uniform diameter of about 150 nm and controllable length up to 5 μm were synthesized via a simple self-assembly method using sodium dodecyl sulfate (SDS) micelles as a template. By changing the relative concentration of the pyrene to SDS molecules, the aspect ratio of the nanorods could be controlled to vary from 1 to 50 or higher. Optical properties of the pyrene nanorods were found to be strongly dependent on the morphology and rod aspect ratio (nanoparticle, short nanorods, and long nanorods or nanowires). As the aspect ratio increases, the optical (i.e., emission peaks, lifetime, and fluorescence anisotropy) features related to isolated pyrene molecules are gradually replaced by those of pyrene aggregates. The present findings provide a simple method for packing small organic molecules into nanostructures of controlled morphologies. It, in turn, offers the possibility of custom tuning their optical properties. This approach is expected to be applicable for assembling organic nanostructures of other molecules.

Acknowledgment. We thank the Chinese Academy of Sciences and the CAS−Croucher Funding Scheme for Joint Laboratories of the Croucher Foundation for financial support. The work in Hong Kong was supported by the Research Grants Council of Hong Kong SAR (Projects No. CityU 2/02C), China.

Supporting Information Available: Fluorescence microscope images for samples A, B, and C; emission spectra for concentrated pyrene solution (1.8×10^{-3} mol L^{-1}) and bulk solid. This material is available free of charge via the Internet at http://pubs.acs.org.

References and Notes

(1) (a) Veinot, J. G. C.; Yan, H.; Smith, S. M.; Cui, J.; Huang, Q. L.; Marks, T. J. *Nano Lett.* **2002**, *2*, 333. (b) Noy, A.; Miller, A. E.; Klare, J. E.; Weeks, B. L.; Woods, B. W.; DeYoreo, J. J. *Nano Lett.* **2002**, *2*, 109.

(2) (a) Kasai, H.; Kamatani, H.; Okada, S.; Oikawa, H.; Matsuda, H.; Nakanishi, H. *Jpn. J. Appl. Phys*. **1996**, *35*, L221. (b) Bushey, M. L.; Nguyen, T. Q.; Nuckolls, C. *J. Am. Chem. Soc.* **2003**, *125*, 8264. (c) Forrest, S. R. *Chem. Rev*. **1997**, *97*, 1793. (d) Hu, D. H.; Yu, J.; Padmanadan, G.; Ramakrishnan, S.; Barbara, P. F. *Nano Lett.* **2002**, *2*, 1121.

(3) (a) Nguyen, T. Q.; Bushey, M. L.; Brus, L. E.; Nuckolls, C. *J. Am. Chem. Soc.* **2002**, *124*, 15051. (b) Fu, H. B.; Xiao, D. B.; Yao, J. N.; Yang, G. Q. *Angew. Chem., Int. Ed*. **2003**, *42*, 2883. (c) Nguyen, T. Q.; Martel, R.; Avouris, P.; Bushey, M. L.; Brus, L.; Nuckolls, C. *J. Am. Chem. Soc.* **2004**, *126*, 5234.

(4) Chiu, J. J.; Kei, C. C.; Perng, T. P.; Wang, W. S. *Adv. Mater*. **2003**, *15*, 1361.

(5) Gong, X. C.; Milic, T.; Xu, C.; Batteas, J. D.; Drain, C. M. *J. Am. Chem. Soc.* **2002**, *124*, 14290.

(6) An, B. K.; Kwon, S. K.; Jung, S. D.; Park, S. Y. *J. Am. Chem. Soc*. **2002**, *124*, 14410.

(7) Lee, J. K.; Koh, W. K.; Chae, W. S.; Kim, Y. R. *Chem. Commun*. **2002**, *2*, 138.

(8) Li, S. Y.; He, L. M.; Xiong, F.; Li, Y.; Yang, G. Q. *J. Phys. Chem. B* **2004**, *108*, 10887.

(9) Zhang, X. J.; Gu, M. M.; Zhang, X. H.; Lee, C. S.; Lee, S. T. Synthesis of Organic Nanostructures and its Morphology Dependence on the Molecular Structures. In preparation.

(10) Tanaka, J. *Bull. Chem. Soc. Jpn.* **1963**, *36*, 1237.

(11) Kelly, M. K.; Etchegoin, P.; Fuchs, D.; Krätschmer, W.; Fostiropoulos, K. *Phys. Rev. B* **1992**, *46*, 4963.

(12) Auweter, H.; Haberkorn, H.; Heckmann, W.; Horn D.; Lüddecke, E.; Rieger, J.; Weiss, H. *Angew. Chem., Int. Ed.* **1999**, *38*, 2188.

(13) Allen, N. S. *Polymer Photochem.* **1984**, *5*, 162.

(14) Trautman, J. K.; Macklin, J. J.; Brus, L. E.; Betzig, E. *Nature* **1994**, *369*, 40.

(15) Betzig, E.; Chichester, R. J. *Science* **1993**, *262*, 1422.

(16) Vanden Bout, D. A.; Kerimo, J.; Higgins, D. A.; Barbara, P. F. *J. Phys. Chem*. **1996**, *100*, 11843.

(17) Kalyanasundaram, K.; Thomas, J. K. *J. Am. Chem. Soc*. **1977**, *99*, 2039.

(18) (a) Honda, C.; Itagaki, M.; Takeda, R.; Endo, K. *Langmuir*, **2002**, *18*, 1999. (b) Jang, J.; Oh, J. H. *Adv. Mater*. **2003**, *15*, 977.